Journal of Theoretical Biology 265 (2010) 202–210

Contents lists available at ScienceDirect

Journal of Theoretical Biology

journal homepage: www.elsevier.com/locate/yjtbi

Can deterministic mechanical size effects contribute to fracture and microdamage accumulation in trabecular bone?

Thomas Siegmund [a,*], Matthew R. Allen [b], David B. Burr [b,c,d]

[a] School of Mechanical Engineering, Purdue University, 585 Purdue Mall, West Lafayette, IN 47907, USA
[b] Department of Anatomy and Cell Biology, MS 5035, Indiana University School of Medicine, 635 Barnhill Dr., Indianapolis, IN 46202, USA
[c] Department of Orthopaedic Surgery, Indiana University School of Medicine, IN 46202, USA
[d] Biomedical Engineering, Indiana University–Purdue University at Indianapolis, IN 46805-1499, USA

ARTICLE INFO

Article history:
Received 12 January 2010
Received in revised form
6 April 2010
Accepted 8 April 2010
Available online 14 April 2010

Keywords:
Microdamage
Biomechanics
Fracture
Fatigue
Size effect

ABSTRACT

Failure of bone under monotonic and cyclic loading is related to the bone mineral density, the quality of the bone matrix, and the evolution of microcracks. The theory of linear elastic fracture mechanics has commonly been applied to describe fracture in bone. Evidence is presented that bone failure can be described through a non-linear theory of fracture. Thereby, deterministic size effects are introduced. Concepts of a non-linear theory are applied to discern how the interaction among bone matrix constituents (collagen and mineral), microcrack characteristics, and trabecular architecture can create distinctively differences in the fracture resistance at the bone tissue level. The non-linear model is applied to interpret pre-clinical data concerning the effects of anti-osteoporotic agents on bone properties. The results show that bisphosphonate (BP) treatments that suppress bone remodeling will change trabecular bone in ways such that the size of the failure process zone relative to the trabecular thickness is reduced. Selective estrogen receptor modulators (SERMs) that suppress bone remodeling will change trabecular bone in ways such that the size of the failure process zone relative to the trabecular thickness is increased. The consequences of these changes are reflected in bone mechanical response and predictions are consistent with experimental observations in the animal model which show that BP treatment is associated with more brittle fracture and microcracks without altering the average length of the cracks, whereas SERM treatments lead to a more ductile fracture and mainly increase crack length with a smaller increase in microcrack density. The model suggests that BPs may be more effective in cases in which bone mass is very low, whereas SERMS may be more effective when milder osteoporotic symptoms are present.

1. Introduction

Recent work in an animal model has documented that two common classes of osteoporosis treatments [bisphosphonates (BPs) and selective estrogen receptor modulators (SERMs)], both of which suppress bone remodeling rate, alter the mechanical properties of trabecular bone and lead to distinctly different microdamage accumulation (Allen et al., 2006). However, they do so by different mechanisms.

BPs (alendronate and risedronate) increase bone mineral density and bone volume (with statistical significance), in part by increasing trabecular thickness (without statistical significance). BPs also change the collagen cross-linking state of the bone tissue (Allen et al., 2008). Such treatment was found to increase ultimate load of trabecular bone (without statistical significance) as well as the stiffness (with statistical significance). BP treatments were found to increase the microcrack density without altering the average length of the cracks.

On the other hand, SERMs (raloxifene) alter bone mechanical properties without significant changes to either bone mineral density or bone volume (Allen et al., 2007), but still increase trabecular thickness (without statistical significance). SERMs change the collagen cross-linking state little. Nevertheless, an increase ultimate load of trabecular bone (but without statistical significance) as well as stiffness (with statistical significance) were found. Interestingly, SERM treatment mainly increases the length of microcracks, with a smaller increase in the crack density.

Changes in turnover do not explain that changes in microdamage accumulation and crack length that are observed experimentally. Experimental results show that BPs and SERMs suppress remodeling to different degrees, but at clinical doses the microcrack density is about the same. Moreover, at these doses, the length of microcracks is significantly longer with

* Corresponding author. Tel.: +1 765 494 9766.
E-mail address: siegmund@purdue.edu (T. Siegmund).

0022-5193/$ - see front matter © 2010 Elsevier Ltd. All rights reserved.
doi:10.1016/j.jtbi.2010.04.009

SERMs than with BPs, yet one might expect, because BPs suppress remodeling to a greater degree, that cracks would not be repaired as quickly and microcracks might be longer. The mechanism underlying these differences is unclear, yet is important to understand with respect to the mechanism by which these agents reduce fracture risk. The purpose of this study was to provide a plausible mathematical explanation for these results.

Following the theories of cellular solids, when a specimen of trabecular bone is subjected to compressive loading individual trabeculae are subjected to bending, and bending deflection then relates to the deformation under the applied compressive load. There is experimental evidence that failure of trabecular bone under compressive loading is related to the formation of zones of localized deformation. Zones of local deformation appear as whitening zones under low magnification imaging, but under high magnification are shown to be delamination type defects aligned with the axis of anisotropy of the bone tissue. The delaminations are fully or partially bridged by collagen fibrils. In addition, crack bridges formed by uncracked ligaments can also be seen. The presence of such mechanisms has been identified to contribute significantly to the resistance to failure both in trabecular (Thurner et al., 2009) and cortical bone (Nalla et al., 2004). The effectiveness of either mechanism is ultimately dependent on the properties of the mineralized collagen fibrils as they are the building blocks of the tissue.

The presence of such fracture processes motivates the use of non-linear fracture models to describe processes underlying failure of individual trabeculae as constituents of cancellous bone. Non-linear fracture mechanics models incorporate a constitutive description of the material separation process during failure. The relevant constitutive description of the material separation process is of a softening type, defined as the relationship between crack surface tractions and material separation. Under monotonic loading, the material separation processes are characterized by a critical traction level, the material strength (σ_0), which is related to the load carrying capacity and the density of the mineralized collagen fibrils. The intrinsic length scale (δ_0) is the material separation distance required such that load transfer between crack faces ceases to exist. This intrinsic length scale is related to the elongation to rupture of the mineralized collagen fibrils (Yeni and Fyhrie, 2003). The product of material strength (σ_0) and intrinsic length scale (δ_0) is the fracture toughness (ϕ_0), i.e. the energy required to create a unit area of new fracture surface. Energy dissipation as characterized by ϕ_0 is then correlated to the stored elastic energy as characterized by E_0, the tissue elastic modulus.

Under cyclic loading, material degradation can occur if the load remains below the monotonic material strength σ_0. The cyclic material separation processes are characterized by an endurance limit ($\Delta\sigma_0$), a critical traction level below which no damage occurs, and a description of the accumulation of damage leading to progressive degradation of the material strength (σ_0) in case the applied load exceeds the endurance limit.

Non-linear fracture mechanics models necessarily introduce a size dependence of failure processes. Such size effects arise naturally as a consequence of the intrinsic length scale (δ_0) and the length measure of the bone architecture. Past studies have previously explored aspects of the size dependence of static failure (Needleman, 1990; Carpinteri, 1991; Gao and Ji, 2003; Bazant, 2005; Taylor, 2008) and fatigue (Kitagawa and Takahashi, 1976; El Haddad et al., 1979; Taylor, 1999; Wang and Siegmund, 2006; Pugno et al., 2007) as related to engineering materials and structures. While such studies commonly focus on configurations dominated by normal stresses, the same type of size effects have also been observed in shear stress dominated configurations (Bazant and Cao, 1986; Morel and Valentine, 1996) as relevant in anisotropic beam-structures. Non-linear fracture models of bone have focused on quasistatic loading of cortical bone (Yeni and Fyhrie, 2003; Ural and Vashishth, 2006; Yang et al., 2006; Kasiri and Taylor, 2008; Ural, 2009). A non-linear fracture model for simulation of failure of cancellous bone was employed by Tomar (2009). This study provides insight into detailed local aspects of trabecular failure based on the detailed analysis of two specific cancellous microstructures. Using the virtual internal bond model, Fang et al. (2010) studied trabecular bone microdamage and determined the relevant contribution of plate and rod-like trabeculae to damage.

Our present study employs a non-linear fracture mechanics model to study failure of trabecular bone. It specifically addresses the hypothesis that the differences in the changes of mechanical properties and microdamage accumulation in cancellous bone treated with BP and SERM could arise as an outcome of size effects, i.e. from synergistic effects between length scales intrinsic to the bone tissue mechanical properties and length scales characteristic of the bone architecture. We first review data from an animal model. A sub-set of the data from the animal model provides the input for the mechanics model. The engineering mechanics model defines equations that predict interaction effects between the material characteristic length scale and the length scales characteristic of the bone architecture. Model predictions are subsequently compared to experimental findings from the animal model.

2. Methods

2.1. Experimental methods

Female beagle dogs (1–2 years old) were treated for 1 year with daily oral doses of drugs commonly used for the treatment of post-menopausal osteoporosis, BP (alendronate, $n=12$/group) and a SERM (raloxifene, $n=12$) (Allen et al., 2006). A separate control group of animals ($n=12$) was treated orally with saline for 12 months.

Following sacrifice, areal bone mineral density (*aBMD*, g/cm^2) of the fourth lumbar vertebrae was measured using a PIXImus II densitometer (Lunar Corp), according to established protocols previously described (Allen et al., 2006). Static histomorphometric measures of fractional bone volume (*BV/TV*, %) and trabecular thickness (*Tb.Th*, μm) were made on the second lumbar vertebrae using a semi-automatic analysis system (Bioquant OSTEO 7.20.10, Bioquant Image Analysis Co.) attached to a microscope (Nikon Optiphot 2). Measurements were made in a 5×5 mm region of interest, 1 mm below the cranial plateau. Trabecular ash weight was used to quantify the mineral content.

Separate vertebrae (third lumbar) were stained en bloc for analysis of bone microdamage, which was assessed microscopically using ultraviolet fluorescence. Measurements included crack density (*Cr.Dn*, #mm^2) and mean crack length (*Cr.Le*, μm).

The biomechanical properties of the fourth lumbar vertebrae were measured using a servohydraulic testing system (MTS 810, MTS Corporation). Compression to failure was performed on saline-soaked specimens in displacement mode (20 mm/min). Specimen stiffness (S), ultimate load (P_{max}), and energy to ultimate load (U_B) are obtained. The modulus of the trabecular bone (E_B), its ultimate stress (σ_B), and energy density to ultimate load (u_B) are obtained as $E_B=[S\times(H/CSA)]$, $\sigma_B=[P_{max}/CSA]$, and $u_B=[U_B/(H\times CSA)]$, respectively, where H and CSA are specimen height and cross-sectional area, respectively, (Turner and Burr, 1993). Subsequently, corresponding trabecular scale properties (trabecular modulus E_T, trabecular strength σ_T, and modulus of toughness u_T) are calculated

by employing the fractional bone volume:

$$E_T = E_B/(BV/TV), \tag{1a}$$

$$\sigma_T = \sigma_B/(BV/TV), \tag{1b}$$

$$u_T = u_B/(BV/TV). \tag{1c}$$

Eq. (1) provides commonly used formulas to obtain first order estimates of trabecular scale properties. The linear relationships between bone level properties and trabecular-level properties with a scaling parameter BV/TV is the simplest assumption and provides upper bound values only. Recent computational studies on trabecular bone failure (Fang et al., 2010) confirm an overall linear relationship between trabecular bone yield strength and BV/TV. As Eq. (1) only predicts overall bone properties it does not account for the details of the bone architecture and local stress enhancements leading to failure, and is not sensitive to architectural changes at constant BV/TV.

Collagen content and cross-linking were evaluated from a core removed from the fourth lumbar vertebrae following mechanical testing. The bone was isolated and powdered in liquid nitrogen, and then lyophilized. Cross-linking was measured using an HPLC protocol previously described (Allen et al., 2008). A remaining portion of the lyophilized bone powder was used to assess native (α) and isomerized (β) forms of C-telopeptide (CTX). The concentration of α-CTX and β-CTX fragments was measured by sandwich assays, and the ratio α/β CTX, which is inversely proportional to collagen maturity, was calculated (Allen et al., 2008).

2.2. Mechanics

We aim to determine the dependence of the failure behavior of trabeculae on the properties of the tissue constituting a trabecula and a relevant size parameter characterizing the cancellous bone architecture.

We first consider monotonic loading. We defined a relationship that correlates the strength of a trabecula (σ_T) to the properties of the trabecular bone tissue emerging from properties of mineralized collagen fibrils (σ_0, δ_0, ϕ_0 and E_0) and size expressed by trabecular thickness ($Tb.Th$). Also, a relationship characterizing the brittleness of the subsequent failure on (σ_0, δ_0, ϕ_0 and E_0) and ($Tb.Th$) is sought. To characterize the dependence of strength on trabecular thickness it is useful to define size in mechanical terms. A length is introduced by the combination of parameters characterizing elastic deformation and material separation (Orowan, 1949). Consider a stress σ carried by a trabecula of dimension $Tb.Th$. Then, the elastic strain energy stored is proportional to the volume of the trabecula $(\sigma^2/2E_0)(Tb.Th)^3$. A critical condition is obtained if failure occurs such that the applied stress reaches the material strength, $\sigma=\sigma_0$. The stored energy at this instance is $W_{el}=(\sigma_0^2/2E_0)(Tb.Th)^3$. The energy dissipated during fracture (W_f), however, would scale with the crack surface area as $W_f=\phi_0(Tb.Th)^2$. When considering a failure process such that all elastic strain energy is dissipated during fracture ($W_{el}=W_f$) a characteristic dimension (L_S) emerges as the ratio of the product of fracture toughness (ϕ_0) and elastic modulus of the tissue (E_0) to the square of the separation strength (σ_0):

$$L_S \sim \frac{\phi_0 E_0}{(\sigma_0)^2} \tag{2}$$

The characteristic dimension (L_S) relates to the extension of the zone of active material degradation. An alternative expression for the characteristic dimension is obtained by considering that fracture toughness (ϕ_0) is proportional to the product of material strength (σ_0) and intrinsic length scale (σ_0) as $\phi_0 \sim \sigma_0\delta_0$. Then, with Eq. (2) the characteristic dimension (L_S) is defined as the ratio of the product of intrinsic length scale (δ_0) and elastic modulus (E_0) to the separation strength (σ_0):

$$L_S \sim \frac{\delta_0 E_0}{\sigma_0}. \tag{3}$$

The definitions of characteristic dimensions of Eqs. (2) and (3) have previously been given by Hillerborg (1983) for concrete and others (Bao and Suo, 1992; Suo et al., 1993; Cox and Marshall, 1994) for crack bridging composites. In the context of bone mechanics, Eq. (2) was previously proposed in Gao et al. (2003) and Ji and Gao (2004) to assess the fracture strength characteristics of mineral platelets. Considering failure of trabecular bone the intrinsic length scale (δ_0), the separation strength (σ_0) and the elastic modulus (E_0) are related to the biomechanical response of the mineralized collagen fibrils. How changes in treatment are thought to affect these parameters is discussed in Section 3.2.2 of this study.

In order to capture the features associated with mechanical failure of a trabecula, size ($Tb.Th$) is now expressed relative to the characteristic dimension (L_S). The normalized size Λ_S is introduced as $\Lambda_S=[(Tb.Th)/L_S]$ (Gao and Chen, 2005). The quantity Λ_S also characterizes the brittleness of the failure process (Carpinteri, 1997; Gao and Chen, 2005).

In a mechanically large trabecula ($\Lambda_S > 1$, and thus $L_S < Tb.Th$) the elastic strain energy stored up to the onset of failure dominates over the energy dissipated during failure, $W_{el} > W_f$. The strength of a trabecula (σ_T) is obtained by comparing W_{el} and W_f. It is dependent on inverse of the normalized size Λ_S and is proportional to material separation strength (σ_0):

$$\sigma_T \sim \sigma_0(\Lambda_S)^{(-1/2)} = \sigma_0\left(\frac{Tb.Th}{L_S}\right)^{(-1/2)} \quad \text{if} \quad \Lambda_S > 1. \tag{4}$$

Consequently, an increase in normalized size leads to decrease in the strength of a trabecula. As $\Lambda_S > 1$, failure is driven by an exceeding availability of stored strain energy. Consequently, the post-peak load behavior is unstable and appears as brittle with a rapid drop in load or even a snap-back response past the ultimate load. For mechanically large trabeculae, the domain of active material degradation is small compared to the structure. This zone is confined to the crack tip and surrounded by an elastic domain. The magnitude of the stresses responsible for crack opening scales as $1/\sqrt{r}$, where (r) is the distance from the crack tip. Such a stress field possesses high stresses at the crack tip, and low stresses remote from the crack tip.

The increase in the strength of trabeculae (σ_T) with decreasing size, Eq. (4), is limited by the material separation strength (σ_0). For trabeculae with $\Lambda_S < 1$ the strength is:

$$\sigma_T \sim \sigma_0 \quad \text{if} \quad \Lambda_S < 1 \tag{5}$$

In such mechanically small trabeculae ($\Lambda_S < 1$, and thus $L_S > Tb.Th$) the energy dissipated during fracture dominates over the elastic strain energy stored up to the onset of failure, $W_{el} < W_f$. The failure process is no longer driven by the stored elastic energy, and can occur only if energy is provided continuously through the external load. As a consequence, the post-peak load behavior of mechanically small trabeculae is ductile, with only a gradual drop in load past the ultimate load. In mechanically small trabeculae, the zone of active material degradation is large and of the order of ($Tb.Th$). Stress fields associated with defects in such mechanically small trabeculae are distributed uniformly throughout, and the stress concentration at the crack tip vanishes.

In fatigue, a cyclically varying applied stress is considered and the amplitude $\Delta\sigma$ of the applied stress characterizes the load. The fatigue limit of a trabecula $\Delta\sigma_T$ defines a load level $\Delta\sigma$ below which no initiation of damage will occur in the trabecula. We aim to establish a relationship that relates $\Delta\sigma_T$ to parameters characterizing the mechanical properties of the tissue ($\Delta\sigma_0$, δ_0,

ϕ_0 and E_0) and the architecture (*Tb.Th*). Also, a characterizing of the subsequent crack growth processes in dependence of ($\Delta\sigma_0$, δ_0, ϕ_0 and E_0) and (*Tb.Th*) is sought. If the load amplitude $\Delta\sigma$ exceeds the endurance limit $\Delta\sigma_T$ then failure is possible. Cyclic failure response can be quantified by the number of cycles to initiation of crack growth (N_{ini}) and the number of total load cycles to failure (N_f).

A generalized description of the size dependence of the fatigue limit is obtained if in the considerations leading to Eqs. (3)–(5) material separation strength σ_0 is substituted with the endurance limit $\Delta\sigma_0$. Following Eq. (3), the characteristic dimension for fatigue failure, L_F, emerges as

$$L_F \sim \frac{\delta_0 E_0}{\Delta\sigma_0} = \frac{\delta_0 E_0}{(\eta\sigma_0)}. \tag{6}$$

The ratio between endurance limit and strength is $\eta=\Delta\sigma_0/\sigma_0$. A second normalized size parameter Λ_F is introduced as $\Lambda_F=(Tb.Th)/L_F$. The ratio $\eta=\Delta\sigma_0/\sigma_0$ is less than one, and consequently $\Lambda_F>\Lambda_S$. Trabeculae appear as mechanically large in fatigue loading if $\Lambda_F>1$, or $L_F<Tb.Th$. Then, the fatigue strength of a trabecula $\Delta\sigma_T$ depends on its size:

$$\Delta\sigma_T \sim \Delta\sigma_0(\Lambda_F)^{(-1/2)} = \Delta\sigma_0\left(\frac{Tb.Th}{L_F}\right)^{(-1/2)} \quad \text{if} \quad \Lambda_F>1 \tag{7}$$

For mechanically large trabeculae, $\Lambda_F>1$, stresses are concentrated at the crack tip, and material degradation under cyclic loading is also localized at the crack tip. Rapid accumulation of damage thus occurs locally at the crack tip and initiation of a defect occurs readily such that the number of load cycles to defect initiation (N_{ini}) is small. Subsequently, a confined zone of material degradation moves through the structure and leaves free crack surfaces in its wake, i.e. the crack extends via a mechanism of crack propagation. Such a process is characterized by a crack advance (Δa) per load cycle (N), and the crack growth rate ($\Delta a/N$) is finite. Fatigue failure of a mechanically large trabecula is consequently dominated by the crack propagation stage, and the number of load cycles to initiate crack growth (N_{ini}) is only a small fraction of the total number of cycles to failure (N_f).

The increase in the trabecular fatigue strength ($\Delta\sigma_T$) with decreasing size, Eq. (7), is limited by the material endurance limit ($\Delta\sigma_0$). For trabeculae with $\Lambda_F<1$ the fatigue strength of the trabecula is thus

$$\Delta\sigma_T \sim \Delta\sigma_0 \quad \text{if} \quad \Lambda_F<1 \tag{8}$$

For mechanically small trabeculae, $\Lambda_F<1$, the change in the characteristics of the stress distribution also changes the response to fatigue loading. Spreading stresses over a larger area reduces the maximum value of the stresses. As a result of the lower stress level, the rate of damage accumulation is lower than the rate of damage accumulation locally at the crack tip in mechanically large trabeculae. The onset of fatigue failure in a mechanically small trabecula is consequently delayed relative to that of a mechanically large trabecula, and the number of cycles to crack growth initiation (N_{ini}) is increased. On the other hand, accumulation of fatigue damage occurs more homogeneously throughout the entire trabecula. Consequently, for $\Lambda_F<1$ the rate of crack extension ($\Delta a/N$) is high, or even instantaneous following initiation.

3. Results

3.1. Experimental data and model input

BP treatment increased the fractional bone volume (*BV/TV*) by 20% relative to the control group (Veh, $p<0.05$). For SERM treatment the increase in the fractional bone volume *BV/TV* was small (3%) and not statistically significant. Changes to *Tb.Th* can be assessed indirectly through calculation from *BV/TV*. For the open-cell cellular architectures of trabecular bone the fractional bone volume relates to *Tb.Th* as $BT/TV=const\times(Tb.Th)^2$ (Gibson and Ashby, 1997). This approach indicates an increase in *Tb.Th* relative to Veh of 9% for BP treatment, but only 1.5% for SERM treatment. Measurements found an increase in *Tb.Th* relative to Veh of 12% for BP, and 8% for SERM. Both changes were found to be below statistical significance. Changes in *BV/TV* are also reflected in bone mineral density data. For BP bone mineral density (*BMD*) increases ~10% ($p<0.05$). SERM treatment did not significantly alter*BMD*. Data on trabecular bone architecture and density are summarized in Table 1. The effects of SERM and BP treatments also were found to differ in their influence on collagen cross-linking. BP treatment was associated with statistically significant increases in collagen cross-linking – both affecting collagen cross-links formed in the presence of enzymes (pyridinoline and deoxypyridinoline) and those that are non-enzymatically formed (e.g., pentosidine). SERM treatment had no statistically significant effect on either pentosidine concentration [*PEN*] or the ratio of non-enzymatic cross-link concentrations [*PYD*]/[*DPD*]. Collagen maturity, inversely related to isomerization expressed as the ratio of α/β C-telopetides, (α/β CTX), also increased significantly with BP treatment and was unchanged with SERM treatment (Table 2).

Table 1
Trabecular histomorphometry for Veh, BP, and SERM treatment.

	BV/TV (%)	*Tb.Th* (μm)		*BMD* (g/cm^2)
		Direct measure	Calculated	
Veh	21.9 ± 0.9	69.4 ± 2.8	69.4	0.33 ± 0.01
BP	26.4 ± 1.0[a]	77.9 ± 4.0	75.6	0.36 ± 0.01[a]
SERM	22.6 ± 1.0	75.2 ± 3.6	70.4	0.31 ± 0.01

Fractional bone volume, *BV/TV*, trabecular thickness *Tb.Th* (direct measure and calculated values from *BV/TV*), and bone mineral density *BMD*. Experimental data following Allen et al. (2006).

[a] Statistically significant difference relative to Veh following BP treatment.

Table 2
Collagen cross linking and collagen maturity for Veh, BP, and SERM treatment.

	[*PYD*]/[*DPD*]	[*PEN*] (mmol/mol collagen)	α/β CTX
Veh	4.63 ± 0.24	1.24 ± 0.08	0.412 ± 0.043
BP	5.45 ± 0.20[a]	1.69 ± 0.04[a]	0.252 ± 0.031[a]
SERM	4.75 ± 0.17	1.27 ± 0.08	0.432 ± 0.025[b]

[*PYD*]/[*DPD*], ratio of pyridinoline and deoxypyridinoline concentration; [*PEN*] pentosidine concentration; α/β CTX collagen maturity.
Experimental data following Allen et al. (2008).

[a] Statistically significant difference relative to Veh following BP treatment.
[b] Statistically significant difference relative to Veh following SERM treatment.

3.2. Model predictions

3.2.1. Parametric model study

Fig. 1 depicts the model predictions of normalized trabecular strength (σ_T/σ_0), Eqs. (4) and (5), and fatigue strength ($\Delta\sigma_T/\Delta\sigma_0$), Eqs. (7) and (8), in dependence of the normalized size. The choice $\eta=(1/3)$was made without loss of generality. The size axes Λ_S, Λ_F are thus not identical, and the axis of Λ_F is shifted to the right relative to Λ_S. A parametric study of changes to strength of trabeculae, σ_T and $\Delta\sigma_T$, with changes in size Λ_S, Λ_F is provided first such that basic cases of property alteration due to size effects are outlined. Each trabecula possesses a value of Λ_S, and for a trabecular bone specimen a range of Λ_S can be defined. Still, an

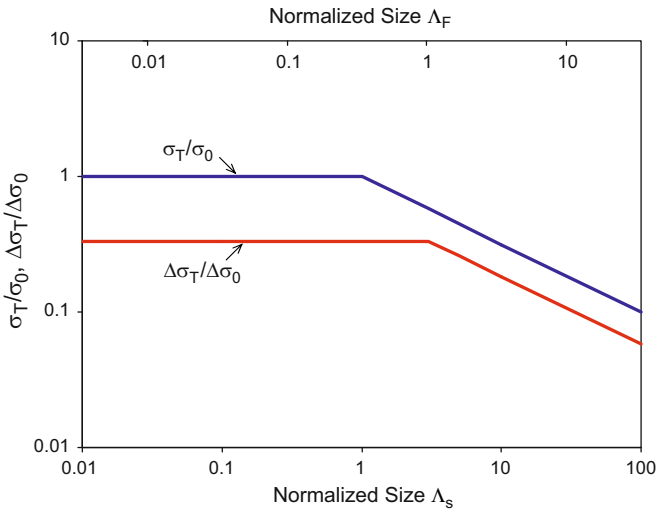

Fig. 1. Predicted dependence of the normalized strength of trabeculae (σ_T/σ_0) and normalized fatigue strength of trabeculae ($\Delta\sigma_T/\sigma_0$) on normalized size Λ_S, Λ_F.

order of magnitude estimate for Λ_S needs to be obtained. Micrographs of loaded trabecular bone samples indicate that delamination cracks with a crack opening of the order of 10 μm remain fully bridged (Thurner et al., 2006, 2007). If one considers a lower bound value for the ratio between the modulus and strength of $E_0/\sigma_0=10$, then a value of L_S on the order of 100 μm emerges such that – considering data for *Tb.Th* in Table 1 – an assumption for the mean value of $\Lambda_S \approx 1$ appears reasonable. For a reference case values of $0.1 < \Lambda_S < 10.0$ are considered such that the range encompasses both mechanically small and large trabeculae. The reference case is denoted as Ref. With $\eta=1/3$ the parameter choice leads to $0.03 < \Lambda_F < 3.33$.

It can be envisioned that changes in size occur without changes to underlying material strength parameters σ_0 and $\Delta\sigma_0$. For one case (C1) an increase of Λ_S by a factor 1.5 is considered while a second case (C2) decreases Λ_S by that same factor. For case C1 the range of normalized size changes to $0.15 < \Lambda_S < 15$. The weakest trabecula is predicted to possess a normalized strength of $\sigma_T/\sigma_0=0.26$ (−18% to Ref for which $\sigma_T/\sigma_0=0.32$). Also, the increase in size increases the sub-set of the size range of Λ_S in the domain $\Lambda_S > 1$. This not only decreases the mean value of σ_T/σ_0 but also increases the overall brittleness. In case C2, the range of size is $0.0667 < \Lambda_S < 6.67$, with the weakest trabecula now predicted to possess strength of $\sigma_T/\sigma_0=0.39$ (+22% to Ref). Decreasing size increases the sub-set of the size range of Λ_S in the domain $\Lambda_S < 1$. The shift of trabeculae into the domain $\Lambda_S < 1$ increases the mean value of σ_T/σ_0 and also decreases the brittleness.

For the evaluation of fatigue strength for case C1, the range of normalized size is $0.05 < \Lambda_F < 5.0$. The trabecula with the lowest fatigue limit possesses $\Delta\sigma_T/\Delta\sigma_0=0.15$ (−18% to Ref for which $\Delta\sigma_T/\Delta\sigma_0=0.18$). The increase in size increases the sub-set of the size range of Λ_F in the domain $\Lambda_F > 1$. This reduces the likelihood that trabeculae would exhibit high resistance to initiation of fatigue damage, and the failure processes under cyclic loading becomes controlled by crack propagation processes following defect formation. For such a situation the crack density *Cr.Dn* would be higher than for the reference case, but the crack length *Cr.Le* of the individual cracks would be reduced. In case C2 the range of normalized size changes to $0.02 < \Lambda_F < 2.2$. The trabecula with the lowest fatigue limit possesses $\Delta\sigma_T/\Delta\sigma_0=0.22$ (+22% to Ref). The decrease in size increases the sub-set of the size range of Λ_F in the domain $\Lambda_F < 1$. This increases the likelihood that trabeculae would exhibit high resistance to initiation of fatigue damage, and the failure processes under cyclic loading becomes controlled by crack initiation and less by crack propagation. Now, the crack density *Cr.Dn* would be lower than for the reference case, but the crack length *Cr.Le* of the individual cracks would be increased.

A second possibility is for the normalized size to change due to changes in σ_0 and $\Delta\sigma_0$. It is considered that one case (C3) increases Λ_S by a factor 1.5 while the other (C4) decreases Λ_S by a factor of 1.5, now through corresponding changes in σ_0. Changes to $\Delta\sigma_0$ follow from $\Delta\sigma_0/\sigma_0=\eta$. Case C3 (modified size range $0.15 < \Lambda_S < 15$) then leads to a range of strength values between $\sigma_T/\sigma_{0,Ref}=1.5$ (+50% to Ref) and $\sigma_T/\sigma_{0,Ref}=0.39$ (+22% to Ref). $\sigma_{0,Ref}$ denotes the value of σ_0 for the scenario without treatment. While strength clearly increases, the increase in size again increases the sub-set of the size range of Λ_S in the domain $\Lambda_S > 1$, and thus leads to an increase the overall brittleness. Case C4 ($0.667 < \Lambda_S < 6.67$), leads to a decreased strength which is predicted to be between $\sigma_T/\sigma_{0,Ref}=0.5$ (−50% to Ref) and $\sigma_T/\sigma_{0,Ref}=0.19$ (−38% to Ref). While strength decreases, the decrease in size increases the sub-set of the size range for which $\Lambda_S < 1$, and thus leads to decreasing brittleness.

Case C3 ($0.05 < \Lambda_F < 5.0$) leads to a range of fatigue strength values between $\Delta\sigma_T/\Delta\sigma_{0,Ref}=0.50$ (+50% to Ref) and $\Delta\sigma_T/\Delta\sigma_{0,Ref}=0.22$ (+22% to Ref). $\Delta\sigma_{0,Ref}$ denotes the value of $\Delta\sigma_0$ for the scenario without treatment. Despite the increase in fatigue strength, case C3 leads to a scenario in which the failure processes under cyclic loading becomes controlled by crack propagation processes following defect formation. Compared to the reference case, the crack density *Cr.Dn* would be increased while the crack length *Cr.Le* of the individual cracks would be reduced. Case C4 ($0.02 < \Lambda_F < 2.2$), leads to a decreased fatigue which is predicted to be in the range of $\Delta\sigma_T/\Delta\sigma_{0,Ref}=0.17$ (−50% to Ref) and $\Delta\sigma_T/\Delta\sigma_{0,Ref}=0.11$ (−38% to Ref). The decrease in size increases the sub-set of the size range for which $\Lambda_S < 1$. Thus, case C4 leads to a scenario in which the failure processes under cyclic loading becomes controlled by crack initiation rather than crack propagation. In such a case the crack density *Cr.Dn* would be lower than for the reference case, but the crack length *Cr.Le* would be increased.

3.2.2. BP and SERM treatment

Changes in collagen cross-link density and maturity determine the mechanical behavior of the mineralized collagen fibril. To date, mechanical properties of the mineralized collagen fibril have mainly been investigated by use of mechanics-based models. Of particular relevance are models that capture the shear mode of deformation in the collagen introduced by the staggered arrangement of the mineral phase (Jäger and Fratzl, 2000; Gao et al., 2003; Kotha and Guzelsu, 2003; Buehler, 2007; Ji, 2008; Siegmund et al., 2008). Following these studies, the shear mode of deformation in the collagen leads to a significant non-linear load–elongation response of the mineralized collagen fibril. The shear mode of deformation shields the mineral phase from high stresses (Gupta et al., 2006). Therefore, the deformation response appears as ductile with a non-linear relationship between load and deformation and a large strain to failure. Collagen cross-linking was shown to reduce the shear mode of deformation and enhance a stretching mode of deformation both in the mineralized collagen fibril (Siegmund et al., 2008) as well as in demineralized collagen fibrils (Buehler, 2008). As a consequence, the relationship between load and deformation becomes increasingly linear with increasing collagen cross-linking. As the shielding of the mineral from load is reduced, the fibril also becomes less ductile. Beyond a critical level of cross-link density the load–elongation response then becomes linear and the fibril appears brittle. Low cross-link densities are associated with an

increase in strength, but again beyond a critical cross-link density strength remains constant.

Fig. 2 schematically depicts the deduced stress–strain response for mineralized collagen fibrils and compares Veh, BP and SERM conditions. Increased non-enzymatic cross-linking and increased collagen maturity as found with BP treatment (Table 2) can thus be linked to an increase in E_0 but would little alter σ_0. Following the reduction of non-linearity of the mechanical response with increasing cross-linking, a proportionally larger change (decrease) in δ_0 than in E_0 would occur. Considering that for BP treatment the trabecular thickness *Tb.Th* increases, this combination of changes results in an increase of the normalized sizes Λ_S and Λ_F. Such a scenario would conform to case C1 as outlined in the previous section. The present model thus predicts that for BP treatment the following trabecular material property changes relative to Veh would occur:

(1) a reduction in strength of trabeculae σ_T;
(2) an increase in brittleness of trabeculae and a reduced u_T;
(3) a lowered resistance to micro-defect formation and thus increased crack density *Cr.Dn*;
(4) an increase in resistance to micro-defect extension and thus shorter length per crack *Cr.Le*; and
(5) an increase in the stiffness of trabeculae (E_T) as the direct consequence of the increase of the stiffness of mineralized collagen fibrils (E_0).

Changes in the properties of trabeculae relate to properties of trabecular bone via Eq. (1). The present model together with Eq. (1) predicts that for BP treatment only a significant increase in *BV/TV* would compensate for the decreases in material properties and lead to the bone structural property changes relative to Veh:

(1) an increase in mechanical strength of trabecular bone σ_B if the increase in *BV/TV* is larger than the decrease in σ_T;
(2) an increase in energy density to ultimate load u_B if the increase in *BV/TV* is larger than the decrease in u_T; and in addition
(3) a significant increase in trabecular bone modulus E_B would occur consequent to increases in both E_T and *BV/TV*.

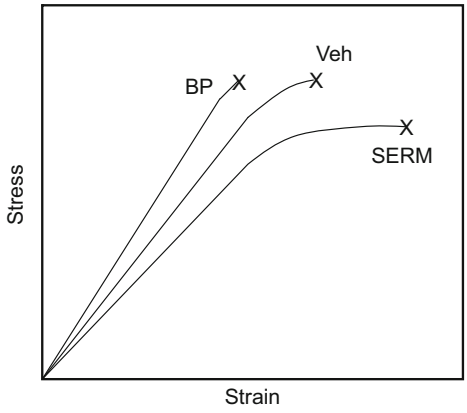

Fig. 2. Schematic drawing of expected characteristics of mineralized collagen fibrils for Veh, BP, and SERM treatments.

For SERM treatment the reduction in collagen maturity (Table 2) can be expected to lead to a small decrease in strength σ_0 and modulus E_0. Relevant changes to the stress–strain response are schematically depicted in Fig. 2. The increase of non-linearity of the mechanical response results in a proportionally larger change (increase) in δ_0 than for σ_0 or E_0. Considering that SERM treatment only changes *Tb.Th* slightly, the normalized sizes Λ_S and Λ_F would tend to decrease. The behavior following SERM treatment would thus correspond to a combination of cases C2 and C4. However, as the changes to σ_0 are minor case C2 might very well dominate. This would result in an increased strength of trabeculae σ_T, decreased brittleness of trabeculae as measured by Λ_S, and increased resistance to micro-defect formation. The present model thus predicts that for SERM treatment the following trabecular material property changes relative to Veh would occur:

(1) an increase in strength of trabeculae σ_T;
(2) a decrease in brittleness of trabeculae and an increased u_T;
(3) an increase in resistance to micro-defect formation and thus decreased crack density *Cr.Dn*, but
(4) a decrease in resistance to micro-defect extension and thus longer length per crack *Cr.Le*; and
(5) a decrease in the stiffness of trabeculae E_T as the direct consequence of the decrease of the stiffness of mineralized collagen fibrils E_0.

For SERM treatment, the present model together with Eq. (1) predicts that the following bone structural property changes relative to Veh would occur because of material property changes in the absence of a significant change in *BV/TV*:

(1) an increase in strength of trabecular bone σ_B as σ_T increases;
(2) an increased u_B as u_T increases; and
(3) a decrease in E_B following a decrease in E_T.

These model predictions are currently based on indirect evidence of changes to σ_0, δ_0, and E_0, thus predictions are provided as

Table 3
Biomechanical properties for Veh, BP, and SERM treatment.

	E_B (MPa)	σ_B (MPa)	u_B (J/mm^3)	E_T (MPa)	σ_T (MPa)	u_T (J/mm^3)
Veh	9.11	0.32	0.0103	41.6 ± 3.6	1.48 ± 0.08	0.047 ± 0.003
BP						
Experiment	11.8	0.36	0.0103	44.9 ± 2.5	1.39 ± 0.07	0.039 ± 0.002
Model trend	↑↑			↑	↓	↓
SERM						
Experiment	11.5	0.37	0.0113	50.9 ± 4.0	1.65 ± 0.10	0.050 ± 0.003[b]
Model trend	↓	↑	↑	↓	↑	↑

Modulus of the trabecular bone E_B, its ultimate stress σ_B, and energy density to ultimate load u_B, as well as trabeculae modulus E_T, trabeculae strength σ_T and trabecular modulus of toughness u_T. Experimental data following Allen et al. (2006). Comparison to trends predicted by the present model. Changes to σ_B and u_B will vary depending on how changes in *BV/TV* compensate for a relative loss in σ_T and u_T.

Table 4
Microdamage accumulation for Veh, BP, and SERM treatment.

	Cr.Dn ($\sharp/mm^2$)	*Cr.Le* (μm)
Veh	0.130 ± 0.04	51.8 ± 4.5
BP		
Experiment	$0.450 \pm 0.08^{a,b}$	56.5 ± 3.4
Model trend	↑	↓
SERM		
Experiment	0.189 ± 0.05	$76.6 \pm 3.0^{a,c}$
Model trend	↓	↑

Mean crack length *Cr.Le*, and crack density *Cr.Dn*.
Experimental data following Allen et al. (2006). Comparison to trends predicted by the present model.

[a] Statistically significant difference relative to Veh following BP or SERM treatment.
[b] Statistically significant difference relative to SERM treatment.
[c] Statistically significant difference relative to BP treatment.

expected trends for trabecular properties and trabecular bone properties. Tables 3 and 4 summarize the model trends.

3.3. Experimental validation

In the animal model, both BP and SERM treatment lead to increase in trabecular bone modulus E_B and trabecular bone strength σ_B. However, only SERM treatment was found to increase the energy density to ultimate load u_B. The trabecular-level properties present a different picture. For both BP and SERM treatment the modulus E_T increased. However, for BP treatment both σ_T and u_T decrease, while the values for these parameters increase for SERM treatment. Table 3 summarizes these findings and compares these to model predictions.

The in vivo accumulation of microdamage is documented in measurements of crack density (*Cr.Dn*) (number of cracks per area) and average crack length (*Cr.Le*). Treatment with BP or with SERM led to different outcomes. For BP, the crack density (*Cr.Dn*) was significantly higher than for vehicle. For SERM, however, crack density (*Cr.Dn*) was only slightly larger than for vehicle. On the other hand, with SERM treatment the average crack lengths (*Cr.Le*) were found to be significantly larger than in vehicle while for BPs crack lengths (*Cr.Le*) were found only to be slightly increased relative to vehicle. Table 4 summarizes these results and compares these to model predictions.

4. Discussion

4.1. Mechanics of size effects

The present study proposes the application of deterministic and energetic size effects in fracture and fatigue to the study of bone failure. Such has been applied to investigations of engineering materials as well as certain biological materials. Alternative to the energetic approach followed here, it has recently been proposed that such size effects could also be studies based on fractal approaches (Carpinteri, 1994). While ongoing debate on the merits of the two approaches exists, the theory of the energetic size effect was chosen for the present study. Probabilistic approaches to fracture and fatigue also can play a role in the studies of size effects (Taylor, 2000). Then, a combined energetic-probabilistic framework could provide enhanced capabilities (Bazant, 2005). The equations describing the size effect, Eqs. (4) and (5), constitute only a basic framework of the approach. More advanced descriptions would also introduce a transition regime between the mechanical large and mechanically small domains such that a domain with a mixed large–small response would exist. In view of the clarity of arguments and the difficulties in identifying further material parameters for such more advanced models, Eqs. (4) and (5) were chosen to provide a basic framework of the proposed novel approach to fracture of cancellous bone. The extension of Eqs. (4) and (5) to fatigue failure was theoretically proposed in Wang and Siegmund (2006). Several features of that model are found in bone in general. A size effect on fatigue as defined by Eqs. (7) and (8) was experimentally shown to exist for dentin (Kruzic and Ritchie, 2006) where size was expressed as initial crack length. Nevertheless, fatigue failure mechanisms in trabecular bone warrant further investigation.

4.2. From bone matrix constituents to bone properties

Mineralized collagen fibrils form the material underlying bone. Trabeculae are small bone tissue elements in the form of plates or rods, which are composed of this protein-based material. In a trabecula the mineralized collagen fibrils are strongly aligned along the long-axis of the bone tissue element. An assembly of a number of trabeculae finally forms the trabecular architecture. Compression failure of trabecular bone has been linked to the formation of shear damage zones within trabeculae (Fyhrie and Schaffler, 1994; Wenzel et al., 1996) and delaminations (Thurner et al., 2006, 2007), which are aligned with the long axis of the individual trabecula. Delaminations have been documented to be bridged by mineralized collagen fibrils, fibril bundles and non-fibrillar organic substances (Thurner et al., 2007). Stretching and rupture of mineralized collagen fibrils thus constitute the major portion of the processes determining trabecular bone failure. The formation of such delaminations and their propagation can be studied using fracture mechanics. High resolution images of permanently deformed trabecular bone (Thurner et al., 2007) indicate that the spatial extension of the material degradation zone can be as large as the trabecular thickness, and is thus significant in relation to the structural dimension of a trabecular strut. These findings suggest that methods of non-linear fracture mechanics are necessary to understand the failure process of interest. It is appropriate to characterize trabeculae as elastic solids in which a finite zone of active material degradation is embedded. The zone of active material degradation is the domain in which stretching and rupture of mineralized collagen fibrils take place. While an exact connection between modification of collagen cross-linking and maturity to the mechanical properties of the mineralized collagen fibril is still missing, the qualitative trends of the dependence of the mechanical properties of the mineralized collagen fibril on collagen cross-linking can be established.

Size effects on trabecular-level strength can be clearly assessed if the geometric dimensions are uniquely measureable, and if material properties can be assessed experimentally. Such favorable conditions are not present in trabecular bone where spatial variations in microarchitecture and in material properties introduce additional variability into the analysis. Furthermore, direct measurements of material properties might not be possible. We can thus not *a-priori* determine if a particular bone is to be classified as mechanically large or small. Nevertheless, several trends on bone failure can still be inferred.

4.3. BP treatment

For conditions of BP treatment, the processes of increasing (*Tb.Th*) and the changes associated with decreasing characteristic dimension (L_S) individually and in combination predict a tendency towards an increase in the normalized size Λ_S. Starting from the

untreated condition an increase in (*Tb.Th*) alone would lead to an increase in mechanical size for trabeculae for which (*Tb.Th*) is larger than (L_S) of the untreated state. For such trabeculae the strength (σ_T) would decrease. Furthermore, as (*Tb.Th*) is increased it is likely that a number of trabeculae will move from the mechanically small to the mechanically large regime, such that the number of trabeculae in the mechanically large regime would increase. Such trabeculae thus no longer possess the maximum possible strength $\sigma_T=\sigma_0$ and would tend to possess enhanced brittleness. Similarly, the decreasing characteristic dimension (L_S) would equally contribute to a decrease in trabecular strength and increase in brittleness even if considered as an independent process. During BP treatment the increase in (*Tb.Th*) and the decrease in characteristic length (L_S) are concurrent processes which reinforce each other, resulting in an even stronger trend of reduced trabecular-level strength (σ_T) and brittleness. For BP conditions both quantities, (σ_T) and (*BV/TV*), change. Although we argue that BP treatment would decrease trabecular-level strength (σ_T), the increase in (*BV/TV*) – in line with (*BMD*) increase – can compensate for the loss in trabecular-level strength such that overall bone strength σ_B will increase. The increase in bone strength found for BP conditions is thus attributed to the increase in the fractional trabecular bone volume *BV/TV* which compensates for the reduced trabecular-level strength σ_T (Allen et al., 2006). Results from experimental studies on animal models under BP treatment conditions are quite well aligned with the model predictions. As BP-treated conditions overall tend to increase mechanical size, the expected post-peak behavior during failure of a trabecula will tend to be rather brittle and allow for little or no energy absorption past the peak load. The experimental study of (Allen et al., 2007) indicates that the trabecular-level modulus of toughness (u_T) of BP-treated dog bone was indeed lower relative to untreated conditions.

For mechanically large trabeculae – a condition for which (L_F) is small and (*Tb.Th*) tends to be large relative to (L_F) – the initiation of crack growth from an existing defect is easier, and (N_{ini}) lower. However, further crack growth would occur slowly. As such, the level of stresses in the structure remains at a high level for a longer period of time, and the formation of additional cracks would remain a possibility. Such a scenario conforms to findings for BP conditions – i.e. where trabeculae would behave as mechanically large – such that the crack density (*Cr.Dn*) is high but crack lengths (*Cr.Le*) are low (Allen et al., 2006). These predictions coincide completely with experimental observations (Table 4).

4.4. SERM treatment

For SERM-treated bone, a different scenario emerges. Now, only an increase the characteristic dimension (L_S) is of concern because (*Tb.Th*) does not change. Again, starting from the untreated condition, an increase in (L_S) would lead to a decrease in the normalized size Λ_S. Furthermore, as (L_S) increases more trabeculae will be in the range $\Lambda_S<1$ and now fall into the mechanically small regime. As SERM-treated conditions overall tend to decrease mechanical size, the expected post-peak behavior during failure of a trabecula will tend to be rather more ductile, as well as lead to an increase in trabecular-level strength. For SERM conditions *BV/TV* remains rather constant, and any increase in bone strength found for SERM conditions is thus attributed to the increase in trabecular-level strength σ_T only. Experimental studies (Allen et al., 2006, 2007) indeed found an 11% increase in trabecular-level strength for SERM treatment. The experimental study of (Allen et al., 2006, 2007) also indicates that the trabecular-level modulus of toughness of SERM-treated dog bone was enhanced relative to untreated conditions, as expected for a more ductile material that allows for energy absorption past the peak load (Table 3).

Mechanically small or mechanically large trabeculae also will respond differently to cyclic fatigue loading. In mechanically small trabeculae – a condition for which (L_F) is large and (*Tb.Th*) tends to be small relative to (L_F) – the initiation of crack growth from an existing defect would be delayed. However, if a crack was initiated, that crack would tend to advance rapidly to greater length. The growth of this crack increases the compliance of the structure leading to a reduction in the overall stress level. This reduction in stress would prevent the formation of further microcracks in that trabecula. Such a scenario aligns with the finding that in SERM conditions – i.e. in a condition tending towards trabeculae behaving as mechanically small – the crack density (*Cr.Dn*) is low but crack lengths (*Cr.Le*) are large (Allen et al., 2006).

5. Conclusion

The model predictions are based on the assumption of a unique value of trabecular width in a given bone specimen. In a given bone the magnitude of trabecular width is certainly not constant. A scenario can be envisioned where the thinnest trabeculae would be mechanically small structures while the thicker trabeculae would be mechanically large structures. It can then be argued that BPs are effective in such a scenario because they increase the load carrying capability of the weakest link in the bone overall while SERMs would not provide such an effect. However, this mechanism in BPs would only be effective as long as the thinnest trabeculae can be considered as mechanically small structures, and points towards the potential existence of a critical trabecular width beyond which a treatment with BPs would be effective while SERMs would not affect bone load carrying capability. As a possible consequence the potential emerges that BPs would be more effective in those cases in which BMD is extremely low, whereas SERMs may be more effective when milder osteoporotic symptoms are present. To obtain quantitatively predictive results with the method proposed here, experiments on failure and fatigue of individual trabeculae need to be conducted and such information be merged with an analysis of size, defect and load distribution within the assembly of trabeculae in the cancellous bone overall.

Acknowledgments

Funding for this study was provided by the Purdue University—Indiana University Collaborative Biomedical Research Initiative CBR3, NIH Grants AR047838 and AR007581 and research grants from The Alliance for Better Bone Health (Procter & Gamble Pharmaceuticals and sanofi-aventis), and Lilly Research Laboratories, as well as an unrestricted grant from Eli Lilly to INSERM. Merck and Co. kindly provided the alendronate. This investigation utilized an animal facility constructed with support from Research Facilities Improvement Program Grant no. C06 RR10601-01 from the National Center for Research Resources, National Institutes of Health.

References

Allen, M.R., Iwata, K., Sato, M., Burr, D.B., 2006. Raloxifene enhances vertebral mechanical properties independent of bone density. Bone 39, 1130–1135, doi:10.1016/j.bone.2006.05.007.

Allen, M.R., Hogan, H.A., Hoobs, W.A., Koivuniemi, A.S., Burr, D.B., 2007. Raloxifene enhances material-level mechanical properties of femoral cortical and trabecular bone. Endocrinology 148, 3908–3913, doi:10.1210/en.2007-0275.

Allen, M.R., Gineyts, E., Leeming, D.J., Burr, D.B., Delmas, P.D., 2008. Bisphosphonates alter trabecular bone collagen cross-linking and isomerization in beagle dog vertebra. Osteoporos Int. 19, 329–337, doi:10.1007/s00198-007-0533-7.

Bao, G., Suo, Z., 1992. Remarks on crack bridging concepts. Appl. Mech. Rev. 45, 355–366, doi:10.1115/1/3119764.
Bazant, Z., Cao, Z., 1986. Size effect of shear failure in prestress concrete beams. ACI J. 83, 260–268.
Bazant, Z., 2005. Scaling of Structural Strength, 2nd ed Elsevier, Butterworth-Heinemann, Oxford, UK, doi:10.1115/1.1584419.
Buehler, M., 2007. Molecular nanomechanics of nascent bone: fibrillar toughening by mineralization. Nanotechnology 18 Article number 295102.
Buehler, M., 2008. Nanomechanics of collagen fibrils under varying cross-link densities: atomistic and continuum studies. J. Mech. Behav. Biomed. Mater. 1, 59–67, doi:10.1016/j.jmbbm.2007.04.001.
Carpinteri, A., 1991. Size-scale transition from ductile to brittle failure—structural response vs. crack growth resistance curve. Int. J. Fract. 51, 175–186, doi:10.1007/BF00033977.
Carpinteri, A., 1994. Fractal nature of material microstructure and size effects on apparent mechanical properties. Mech. Mater. 18, 89–101, doi:10.1016/0167-6636(94)00008-5.
Carpinteri, A., 1997. Structural Mechanics: A Unified Approach. Chapman & Hall, London.
Cox, B.N., Marshall, D.B., 1994. Concepts for bridged cracks in fracture and fatigue. Acta Metall. Mater. 42, 341–363, doi:10.1016/0956-7151(94)90492-8.
El Haddad, M., Topper, T., Smith, K., 1979. Prediction of non-propagating cracks. Eng. Fract. Mech. 11, 573–584, doi:10.1016/0013-7944(79)90081-X.
Fang, G., Ji, B.H., Liu, X.S., Guo, X.E., 2010. Quantification of trabecular bone microdamage using the virtual internal bond model and the individual trabecular segmentation technique. Comput. Meth. Biomech. Biomed. Eng., iFirst article, doi:10.1080/10255840903405660.
Fyhrie, D.P., Schaffler, M.B., 1994. Failure mechanisms in human vertebral cancellous bone. Bone 15, 105–109, doi:10.1016/8756-3282(94)90900-8.
Gao, H.J., Ji, B.H., Jäger, I.L., Arzt, E., Fratzl, P., 2003. Materials become insensitive to flaws at nanoscale: lessons from nature. Proc. Natl. Acad. Sci. 100, 5597–5600, doi:10.1073/pnas.0631609100.
Gao, H.J., Ji, B.H., 2003. Modeling fracture in nanomaterials via a virtual internal bond method. Eng. Fract. Mech. 70, 1777–1791, doi:10.1016/S0013-7944(03)00124-3.
Gao, H., Chen, S., 2005. Flaw tolerance in a thin strip under tension. J. Appl. Mech. 72, 732–737, doi:10.1115/1.1988348.
Gibson, L.J., Ashby, M.F., 1997. Cellular Solids, 2nd ed Cambridge University Press, Cambridge, UK.
Gupta, H.S., Sta, J., Wagermaier, W., Zaslansky, P., Boesecke, P., Fratzl, P., 2006. Cooperative deformation of mineral and collagen in bone at the nanoscale. Proc. Natl. Acad. Sci. 103, 17741–17746, doi:10.1073/pnas.0604237103.
Hillerborg, A., 1983. Analysis of one single crack. In: Wittmann, F.H. (Ed.), Fracture Mechanics of Concrete. Elsevier, Amsterdam, pp. 223–249.
Jäger, I., Fratzl, P., 2000. Mineralized collagen fibrils: a mechanical model with a staggered arrangement of mineral particle. Biophys. J. 79, 1737–1746, doi:10.1016/S0006-3495(00)76426-5.
Ji, B.H., Gao, H., 2004. Mechanical properties of nanostructures biological materials. J. Mech. Phys. Solids 52, 1963–1990, doi:10.1016/j.jmps.2004.03.006.
Ji, B.H., 2008. A study of the interface strength between protein and mineral in biological materials. J. Biomech. 41, 259–266, doi:10.1016/j.jbiomech.2007.09.022.
Kasiri, S., Taylor, D., 2008. A critical distance study of stress concentration in bone. J. Biomech. 41, 603–609, doi:10.1016/j.jbiomech.2007.10.003.
Kitagawa, H., Takahashi, S., 1976. Applicability of fracture mechanics to very small cracks or cracks in the early stage. In: Proceedings of the Second International Conference on Mechanical Behavior of Materials. ASM, pp. 627–631.
Kotha, S.P., Guzelsu, N., 2003. Effect of bone mineral content on the tensile properties of cortical bone: experiments and theory. J. Biomech. Eng. 125, 785–793, doi:10.1115/1.1631586.
Kruzic, J.J., Ritchie, R.O., 2006. Kitagawa–Takahashi diagrams define the limiting conditions for cyclic fatigue failure in human dentin. J. Biomed. Mater. Res. A 79, 747–751, doi:10.1002/jbm.a.30939.
Morel, S., Valentine, G., 1996. Size effect in crack shear strength of wood. J. Phys. IV C6 (6), 385–394.
Nalla, R.K., Kruzic, J.J., Ritchie, R.O., 2004. On the origin of the toughness of mineralized tissue: microcracking or crack bridging? Bone 34 790–798, doi:10.1016/j.bone.2004.02.001.
Needleman, A., 1990. An analysis of decohesion along an imperfect interface. Int. J. Fract. 42, 21–40, doi:10.1007/BF00018611.
Orowan, E., 1949. Fracture and strength of solids. Rep. Prog. Phys. 12, 185–232, doi:10.1088/0034-4885/12/1/309.
Pugno, N., Cornetti, P., Carpinteri, A., 2007. New unified laws in fatigue: from the Woehler's to the Paris regime. Eng. Fract. Mech. 74, 595–601, doi:10.1016/j.engfracmech.2006.07.009.
Siegmund, T., Allen, M.R., Burr, D.B., 2008. Failure of mineralized collagen fibrils: modeling the role of cross-linking. J. Biomech. 41, 1427–1435, doi:10.1016/j.jbiomech.2008.02.017.
Suo, Z., Ho, S., Gong, X., 1993. Notch ductile-to-brittle transition due to localized inelastic band. J. Eng. Mater. Technol., 319–327, doi:10.1115/1.2904225.
Taylor, D., 1999. Geometrical effects in fatigue: a unifying theoretical model. Int. J. Fatigue 21, 413–420, doi:10.1016/S0142-1123(99)00007-9.
Taylor, D., 2000. Scaling effects in the fatigue strength of bones from different animals. J. Theor. Biol. 206, 299–306, doi:10.1006/jtbi.2000.2125.
Taylor, D., 2008. The theory of critical distances. Eng. Fract. Mech. 75, 1696–1705, doi:10.1016/j.engfracmech.2007.04.007.
Thurner, P.J., Wyss, P., Voide, R., Stauber, M., Stampanoni, M., Sennhauser, U., Müller, R., 2006. Time-lapsed investigation of three-dimensional failure and damage accumulation in trabecular bone using synchrotron light. Bone 39, 289–299, doi:10.1016/j.bone.2006.01.147.
Thurner, P.J., Erickson, B., Jungmann, R., Schriock, Z., Weaver, J.C., Fantner, G.E., Schitter, G., Morse, D.E., Hansma, P.K., 2007. High-speed photography of compressed human trabecular bone correlates whitening to microscopic damage. Eng. Fract. Mech. 74, 1928–1941, doi:10.1016/j.engfracmech.2006.05.024.
Thurner, P.J., Erickson, B., Turner, P., Jungmann, R., Lelujian, J., Procter, A., Weaver, J.C., Schitter, G., Morse, D.E., Hansma, P.K., 2009. The effect of NaF in vitro on the mechanical and material properties of trabecular and cortical bone. Adv. Mater. 21, 451–457, doi:10.1002/adma.200801204.
Tomar, V., 2009. Insights into the effects of tensile and compressive loadings on microstructure dependent fracture of trabecular bone. Eng. Fract. Mech. 74, 1928–1941, doi:10.1016/j.engfracmech.2008.12.013.
Turner, C.H., Burr, D.B., 1993. Basic biomechanical measurements of bone—a tutorial. Bone 14, 595–608, doi:10.1016/8756-3282(93)90081-K.
Ural, A., 2009. Prediction of Colles' fracture load in human radius using cohesive finite element modeling. J. Biomech. 42, 22–28, doi:10.1016/j.jbiomech.2008.10.011.
Ural, A., Vashishth, D., 2006. Cohesive finite element modeling of age-related toughness loss in human cortical bone. J. Biomech. 39, 2974–2982, doi:10.1016/j.jbiomech.2005.10.018.
Wang, B., Siegmund, T., 2006. A computational analysis of size effects in fatigue failure. Model. Simul. Mater. Sci. Eng. 14, 775–787, doi:10.1088/0965-0393/14/4/017.
Wenzel, T.E., Schaffler, M.B., Fyhrie, D.P., 1996. In vivo trabecular microcracks in human vertebral bone. Bone 19, 89–95, doi:10.1016/8756-3282(96)88871-5.
Yang, Q.D., Cox, B.N., Nalla, R.K., Ritchie, R.O., 2006. Fracture length scales in human cortical bone: the necessity of nonlinear fracture models. Biomaterials 27, 2095–2113, doi:10.1016/j.biomaterials.2005.09.040.
Yeni, Y., Fyhrie, D.P., 2003. A rate-dependent microcrack-bridging model that can explain the strain rate dependency of cortical bone apparent yield strength. J. Biomech. 36, 1343–1353, doi:10.1016/S0021-9290(03)00122-2.